INTERNATIONAL JOURNAL OF CHEMICAL REACTOR ENGINEERING

Volume 9 2011 *Article* A113

Melting Effect on Unsteady Hydromagnetic Flow of a Nanofluid Past a Stretching Sheet

Ali J. Chamkha* A.M. Rashad†

Eisa Al-Meshaiei‡

*The Public Authority for Applied Education and Training, achamkha@yahoo.com

†South Valley University, am_rashad@yahoo.com

‡The Public Authority for Applied Education and Training, meshaiei@yahoo.com

ISSN 1542-6580

Melting Effect on Unsteady Hydromagnetic Flow of a Nanofluid Past a Stretching Sheet*

Ali J. Chamkha, A.M. Rashad, and Eisa Al-Meshaiei

Abstract

This paper considers unsteady, laminar, boundary-layer flow with heat and mass transfer of a nanofluid along a horizontal stretching plate in the presence of a transverse magnetic field, melting and heat generation or absorption effects. The model used for the nanofluid incorporates the effects of Brownian motion and thermophoresis. The governing partial differential equations are transformed into a set of non-similar equations and solved numerically by an efficient implicit, iterative, finite-difference method. A parametric study illustrating the influence of various physical parameters is performed. Numerical results for the steady-state velocity, temperature and nanoparticles volume fraction profiles as well as the time histories of the skin-friction coefficient, Nusselt number and the Sherwood number are presented graphically and discussed.

KEYWORDS: unsteady boundary-layer, melting effect, magnetohydrodynamics, nanofluids

*Ali J. Chamkha is in the Manufacturing Engineering Department, The Public Authority for Applied Education and Training, Shuweikh 70654, Kuwait.
A.M. Rashad is in the Department of Mathematics, South Valley University, Faculty of Science, Aswan, Egypt.
Eisa Al-Meshaiei is in the Manufacturing Engineering Department, The Public Authority for Applied Education and Training, Shuweikh 70654, Kuwait.

1. Introduction

Heat transfer accompanied by melting effect has received much attention in recent years because of its important applications in permafrost melting, frozen ground thawing, liquid polymer extrusion, casting and welding processes as well as phase change material (PCM). In manufacturing processes such as hot extrusion, a material such as metals, polymers, ceramics and others is pushed or drawn through a die of the desired cross-section to produce different types of objects. The melting effect is important in hot extrusion or hot working process since it is done above the material's re-crystallization temperature to keep the material from work hardening and to make it easier to push the material through the die. Also, in the permafrost research, the melting effect plays an important role in the problems of permafrost melting and frozen ground thawing. According to the analysis of Walker (2007), the phenomenon of permafrost degradation in Arctic Alaska is very critical due to global warming and this result accelerates the greenhouse effect. Many studies have been reported concerning the melting process by heat convection mechanism. For example, Kazmierczak, et al. (1987) presented similarity solutions to analyze the melting phenomenon from a vertical plate in porous medium induced by forced convection of a dissimilar fluid. Hassanien and Bakier (1991) studied the melting effect in mixed convection flow from a horizontal flat plate embedded in a porous medium. Bakier (1997) studied the melting effect on a plate with aiding and opposing flows for an arbitrary wall temperature. Gorla, et al. (1999) changed the arbitrary wall temperature by a uniform wall temperature at the solid-liquid interface to analyze the velocity and temperature fields for aiding flow conditions. Cheng and Lin (2007) examined the melting effect on mixed convective heat transfer from a porous vertical plate in liquid-saturated porous medium with aiding and opposing external flows. Cheng and Lin (2008) also examined transient mass transfer in mixed convective heat flow with melting effect from a vertical plate in a liquid-saturated porous medium in the presence of aiding external flow. Bakier, et al. (2008) studied hydromagnetic heat transfer by mixed convection from a vertical plate in a liquid-saturated porous medium in the presence of melting effect. Recently, Chamkha, et al. (2010) considered the effects of melting and heat generation or absorption on steady mixed convection from a radiate vertical wall embedded in a non-Newtonian power-law fluid-saturated porous medium for aiding and opposing external flows.

On other hand, it is well known that conventional heat transfer fluids, including oil, water, and ethylene glycol mixture are poor heat transfer fluids, since the thermal conductivity of these fluids plays an important role on the heat transfer coefficient between the heat transfer medium and the heat transfer surface. An innovative technique for improving heat transfer by using ultra fine

solid particles in the fluids has been used extensively during the last several years. A nanofluid, which is a term introduced by Choi (1995), is a base fluid with suspended metallic nano-scale particles called nanoparticles. Because traditional fluids used for heat transfer applications such as water, mineral oils and ethylene glycol have a rather low thermal conductivity, nanofluids with relatively higher thermal conductivities have attracted enormous interest from researchers due to their potential in enhancement of heat transfer with little or no penalty in pressure drop. Daungthongsuk and Wongwises (2008) studied the influence of thermophysical properties of nanofluids on the convective heat transfer and summarized various models used in literature for predicting the thermophysical properties of nanofluids. The problem of thermal instability in a porous medium layer saturated by a nanofluid was investigated by Nield and Kuznetsov (2009). Abu-Nada and Oztop (2009) studied effects of inclination angle on natural convection in enclosures filled with Cu-water nanofluid. Nield and Kuznetsov (2009) suggested natural convective boundary-layer flow of a nanofluid past a vertical plate. Chamkha, et al. (2011) studied mixed convection MHD flow of a nanofluid past a stretching permeable surface in the presence of Brownian motion and thermopherosis effects. Chamkha, et al. (2011) also analyzed natural convection past a sphere embedded in a porous medium saturated by a nanofluid. Gorla, et al. (2011) studied steady boundary layer flow of a nanofluid on a stretching circular cylinder in a stagnant free stream. Rana and Bhargava (2011) analyzed the development of steady boundary-layer flow and heat transfer for different types of nanofluids along a vertical plate with temperature-dependent heat source or sink. Hamad (2011) examined convective flow and heat transfer of an incompressible viscous nanofluid past a semi-infinite vertical stretching sheet in the presence of a magnetic field.

The objective of this paper is to study hydromagnetic, forced convection, boundary-layer flow of a nanofluid over a horizontal stretching plate in the presence of a transverse magnetic field and melting and heat generation or absorption effects. The model used for the nanofluid incorporates the effects of Brownian motion and thermophoresis.

2. Problem Formulation

Consider unsteady, incompressible, hydromagnetic, forced convection, boundary-layer flow of an electrically-conducting and heat-generating nanofluid over a flat plate stretched with a linear velocity with the tangential coordinate x. The flow configuration is shown in Fig. 1 with the corresponding Cartesian coordinates (x,y) in horizontal and vertical directions, respectively, with the positive y-axis pointing towards the external flow. A uniform magnetic field is applied in the transverse direction y normal to the plate.

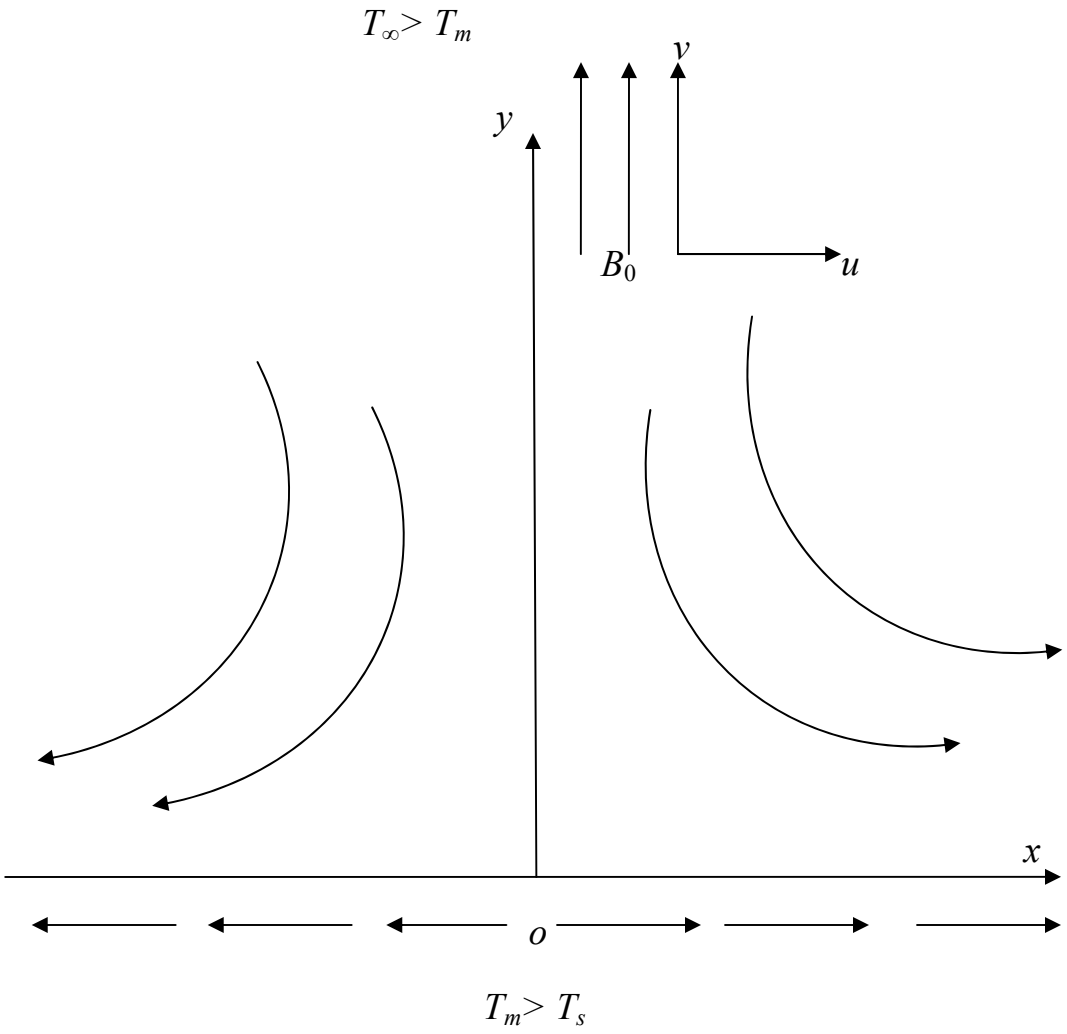

Figure 1: Physical model and coordinate system

It is assumed that the temperature of the melting surface is T_m, while the temperature at the free stream is T_∞ such that $T_\infty > T_m$. Further, it is assumed that the magnetic Reynolds number is small so that the induced magnetic field is neglected and that the heat generation or absorption effect is based on the difference between the local and melting temperatures. The governing equations for this investigation are based on the balance laws of mass, linear momentum, energy and nanoparticles volume fraction modified to account for the presence of

the melting, magnetic field and the heat generation or absorption effects. These can be written as (see, Chamkha (1998));

$$\frac{\partial u}{\partial x}+\frac{\partial v}{\partial y}=0, \tag{1}$$

$$\frac{\partial u}{\partial t}+u\frac{\partial u}{\partial x}+v\frac{\partial u}{\partial y}=\upsilon\frac{\partial^2 u}{\partial y^2}-\frac{\sigma}{\rho_f}B_0^2 u, \tag{2}$$

$$\frac{\partial T}{\partial t}+u\frac{\partial T}{\partial x}+v\frac{\partial T}{\partial y}=\alpha\frac{\partial^2 T}{\partial y^2}+\chi\left[D_B\frac{\partial C}{\partial y}\frac{\partial T}{\partial y}+\frac{D_T}{T_\infty}\left(\frac{\partial T}{\partial y}\right)^2\right]+\frac{Q_0}{(\rho c)_p}(T-T_m), \tag{3}$$

$$\frac{\partial C}{\partial t}+u\frac{\partial C}{\partial x}+v\frac{\partial C}{\partial y}=D_B\frac{\partial^2 C}{\partial y^2}+\left(\frac{D_T}{T_\infty}\right)\frac{\partial^2 T}{\partial y^2}, \tag{4}$$

where t, x and y represent time, tangential distance, and transverse or normal distance, respectively. u, v, T and C are the fluid tangential velocity, normal velocity, temperature, and nanoparticles volume fraction, respectively. υ, ρ_f, σ and B_0 are the kinematic viscosity of the base fluid, density of the base fluid, electrical conductivity, and the magnetic induction, respectively. $\alpha = k/(\rho c)_f$ and $\chi = (\rho c)_p/(\rho c)_f$ are the thermal diffusivity and the ratio of heat capacities, respectively. k, $(\rho c)_f$ and $(\rho c)_p$ are thermal conductivity, heat capacity of the fluid and the effective heat capacity of nanoparticles material, respectively. Q_0 is the heat generation or absorption coefficient. It should be mentioned that positive values of Q_0 indicate heat generation (source) and negative values of Q_0 correspond to heat absorption (sink). D_B and D_T are the Brownian diffusion coefficient and the thermophoretic diffusion coefficient, respectively.

The corresponding initial and boundary conditions for this problem can be written as:

$$u(0,x,y)=ax,\ T(0,x,y)=T_m,\ C(0,x,y)=C_w, \tag{5a}$$
$$u(t,x,0)=ax,\ T(t,x,0)=T_m,\ C(t,x,0)=C_w,$$
$$k\frac{\partial T(t,x,0)}{\partial y}=\rho\left[\lambda+C_s(T_m-T_s)\right]v(t,x,0),$$

$$u(t,x,\infty)=0,\ T(t,x,\infty)=T_\infty,\ C(t,x,\infty)=C_\infty. \tag{5b}$$

where a is a constant and C_s and λ are the heat capacity of the solid surface, the latent heat of the fluid, respectively. T_s, T_m and C_w are the surface temperature, melting temperature and the wall nanoparticles volume fraction, respectively. T_∞ and C_∞ are the temperature and nanoparticles volume fraction, respectively. Equation (5) states that the heat conducted to the melting surface is equal to the heat of melting plus the sensible heat required to raise the solid surface temperature T_s to its melting temperature T_m (see Epstein and Cho (1976)). The detailed derivation of Eq. (5) can be found in the paper by Roberts (1958).

It is convenient to non-dimensionalize and transform Eqs. (1) through (4) by using

$$t = \tau / a,\ y = 2\sqrt{\upsilon t}\,\eta,\ u = axf'(\tau,t),\ v = -2a\sqrt{\upsilon t}\,f(\tau,\eta),$$
$$T = T_m + (T_\infty - T_m)\theta(\tau,\eta),\ C = C_w + (C_\infty - C_w)\phi(\tau,\eta). \quad (6)$$

Substituting Eqs. (6) into Eqs. (1) through (4) yields:

$$f''' + 2\eta f'' - 4\tau\frac{\partial f'}{\partial \tau} + 4\tau\left(ff'' - f'^2 - Ha^2 f'\right) = 0, \quad (7)$$

$$\frac{1}{\Pr}\theta'' + Nb\,\phi'\theta' + 2\eta\theta' - 4\tau\frac{\partial \theta}{\partial \tau} + 4\tau\left(f\theta' + Q\theta\right) + Nt\,\theta'^2 = 0, \quad (8)$$

$$\phi'' + Le\left(2\eta\phi' - 4\tau\frac{\partial \phi}{\partial \tau} + 4\tau f\phi'\right) + \frac{Nt}{Nb}\theta'' = 0. \quad (9)$$

where Eq. (1) is identically satisfied. In Eqs. (7)-(9), a prime indicates differentiation with respect to η and the parameters $Ha = B_0\sqrt{\sigma/(\rho a)}$, $Q = Q_0/(\rho C_p a)$, $M = \dfrac{C_p(T_\infty - T_m)}{\left(\lambda + C_s(T_m - T_s)\right)}$, $Nb = \dfrac{(\rho c)_p D_B (C_\infty - C_w)}{(\rho c)_f \upsilon}$, $Nt = \dfrac{(\rho c)_p D_T (T_\infty - T_m)}{(\rho c)_f \upsilon T_\infty}$, $Le = \alpha / D_B$ and $\Pr = \upsilon/\alpha$ are the Hartmann number, dimensionless heat generation or absorption coefficient, Stefan number or melting parameter, Brownian motion parameter, thermophoresis, Lewis number and the Prandtl number, respectively. It should be mentioned that in the absence of the melting, Brownian motion and thermophoresis effects (M=Nb=Nt=0) the equations reported by Chamkha (1998) are recovered.

The transformed initial and boundary conditions become:

$$f'(0,\eta)=1,\ \theta(0,\eta)=0,\ \phi(0,\eta)=0,\ f'(\tau,0)=1,\ \theta(\tau,0)=0, \tag{10a}$$
$$\phi(\tau,0)=0,\ 4\tau\,\mathrm{Pr} f(\tau,0)+M\,\theta'(\tau,0)=0,\ f'(\tau,\infty)=0,$$

$$\theta(\tau,\infty)=1,\ \phi(\tau,\infty)=1. \tag{10b}$$

Of special significance for this type of flow and heat transfer situation are the skin-friction coefficient, Nusselt number and the Sherwood number. These physical parameters can be defined in dimensionless form as:

$$C_f=-\frac{\mu(\partial u/\partial y)_{y=0}}{\mu(ax)/2\sqrt{\upsilon t}}=-f''(\tau,0) \quad , \tag{11}$$

$$Nu=-\frac{k(\partial T/\partial y)_{y=0}}{k(T_\infty-T_m)/2\sqrt{\upsilon t}}=-\theta'(\tau,0), \tag{12}$$

$$Sh=-\frac{D_B(\partial C/\partial y)_{y=0}}{D_B(C_\infty-C_w)/2\sqrt{\upsilon t}}=-\phi'(\tau,0), \tag{13}$$

3. Numerical Method

The initial-value problem represented by Eqs. (7) through (10) is nonlinear and possesses no analytical solution. Therefore, a numerical solution is sought for this problem. The standard implicit, iterative, finite-difference method discussed by Blottner (1970) has proven to be adequate and accurate for this type of problems and therefore, it is chosen for the solution of Eqs. (7)-(9) subject to Eqs. (10). The computational domain is divided into 196 by 196 nodes in the τ and η directions, respectively. Since the changes in the dependent variables are large in the immediate vicinity of the plate while these changes decrease greatly as the distance above the plate increases, variable step sizes in the η direction are used. For the same reason, variable step sizes in the τ direction are also employed. The initial step sizes employed were $\Delta\eta_1$ = 0.001 and $\Delta\tau_1$= 0.001 and the growth factors were K_η = 1.03 and K_τ = 1.03 such that $\Delta\eta_n = K_\eta\,\Delta\eta_{n-1}$ and $\Delta\tau_m = K_\tau\,\Delta\tau_{m-1}$. The convergence criterion used was based on the relative difference between the current and the previous iterations which was set to 10^{-5} in the present work. For

more details on the numerical procedure, the reader is advised to read the paper by Blottner (1970).

4. Results and Discussion

Figures 1 through 20 represent typical numerical results based on the solution of Eqs. (7)-(10). These results are obtained to illustrate the influence of the Hartmann number, Stefan number or melting parameter, Brownian motion parameter, thermophoresis parameter, Lewis number, and the heat generation or absorption coefficient on the profiles of the fluid tangential velocity and temperature and the nanoparticles volume fraction as well as the transient developments of the skin-friction coefficient C_f, Nusselt number Nu and the Sherwood number Sh. It should be mentioned that in all the results, Pr=0.007 corresponding to liquid metal gallium.

Figures 2(a)-2(c) show typical unsteady-state fluid tangential velocity f', temperature θ and nanoparticles volume fraction ϕ for various values of the magnetic Hartmann number Ha, respectively. Application of a transverse magnetic field normal to the flow direction gives rise to a resistive drag-like force acting in a direction opposite to that of the flow. This has a tendency to reduce the fluid tangential velocity and its temperature and consequently, the nanoparticles volume fraction. This is indicative from the decreases in f', θ, and ϕ as Ha increases shown in Figures 1(a)-(c), respectively.

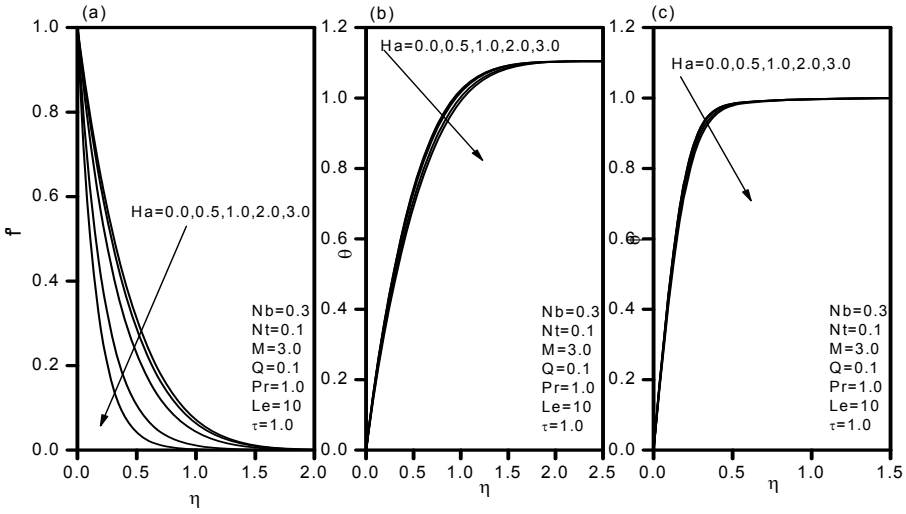

Figure 2: Effects of Ha on the (a) velocity, (b) temperature, (c) volume fraction profiles

Figures 3-5 illustrate the transient development of the skin-friction coefficient C_f, Nusselt number Nu and the Sherwood number Sh for different values of Ha, respectively. As mentioned before, increases in Ha cause respective decreases in f', θ, and ϕ. This results in increasing the slope of the tangential velocity and decreasing the slopes of the temperature and nanoparticles volume fraction. This has the direct effect of increasing C_f and decreasing both *Nu* and *Sh* due to increases in *Ha* as depicted in Figures 2-4, respectively. In addition, it is observed that, in general, all of the local skin-friction coefficient, local Nusselt number and the local Sherwood number increase as the dimensionless time τ increases.

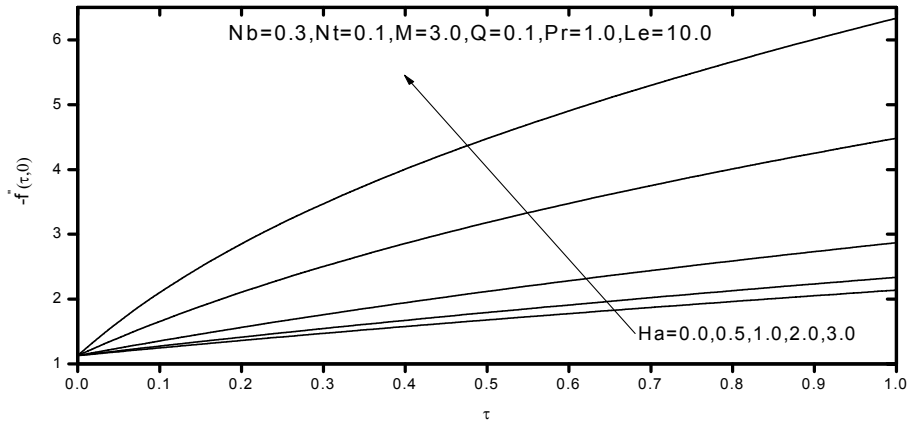

Figure 3: Effects of *Ha* on the skin-friction coefficient

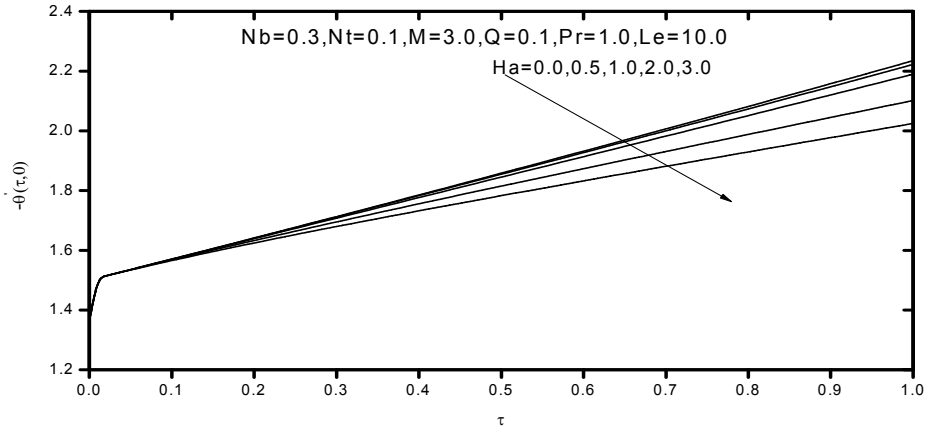

Figure 4: Effects of *Ha* on the Nusselt number

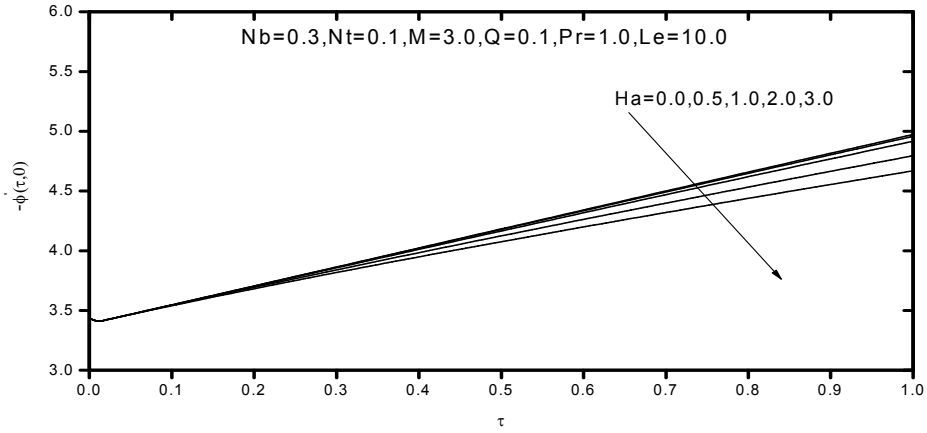

Figure 5: Effects of *Ha* on the Sherwood number

Figures 6(a)-6(c) present the influence of the Stefan number or melting parameter M on the unsteady-state tangential velocity, temperature and nanoparticles volume fraction profiles, respectively. It is obvious that increasing the melting parameter M causes higher restriction to the fluid flow which, in turn, slows its motion and causes increases in the temperature and volume fraction profiles. This is accompanied by respective decreases in the boundary-layer thicknesses of velocity, temperature and nanoparticles volume fraction.

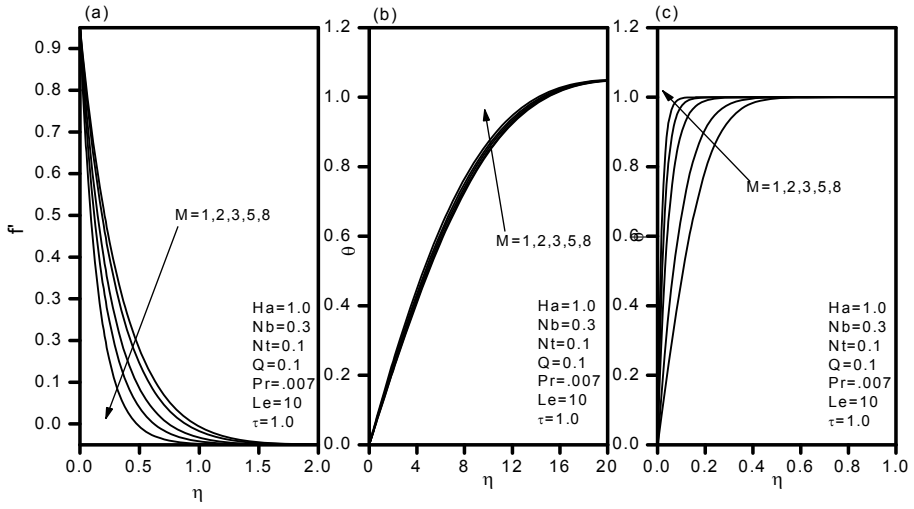

Figure 6: Effects of M on the (a) velocity, (b) temperature, (c) volume fraction profiles

Figures 7-9 depict the influence of the Stefan number or melting parameter M on the time histories of the skin-friction coefficient, Nusselt number and the Sherwood number, (C_f, Nu and Sh), respectively. It is clear that increasing the value of the melting parameter M yields increases in all of the local skin-friction coefficient, local Nusselt number and the local Sherwood number.

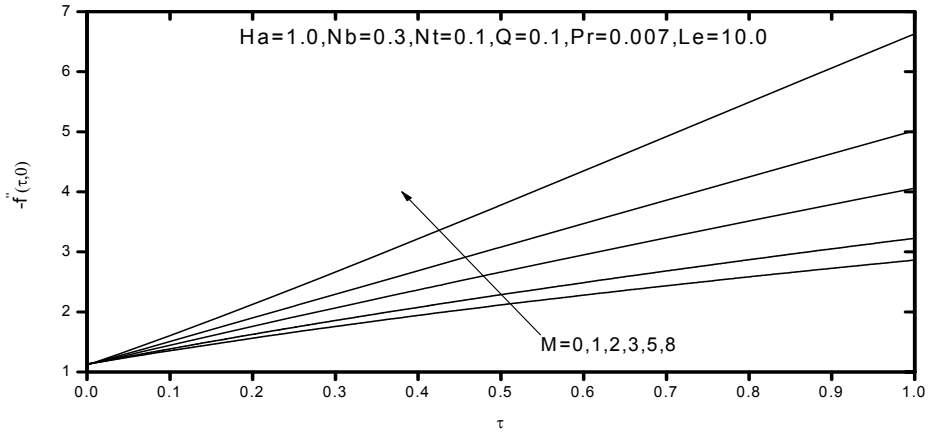

Figure 7: Effects of M on the skin-friction coefficient

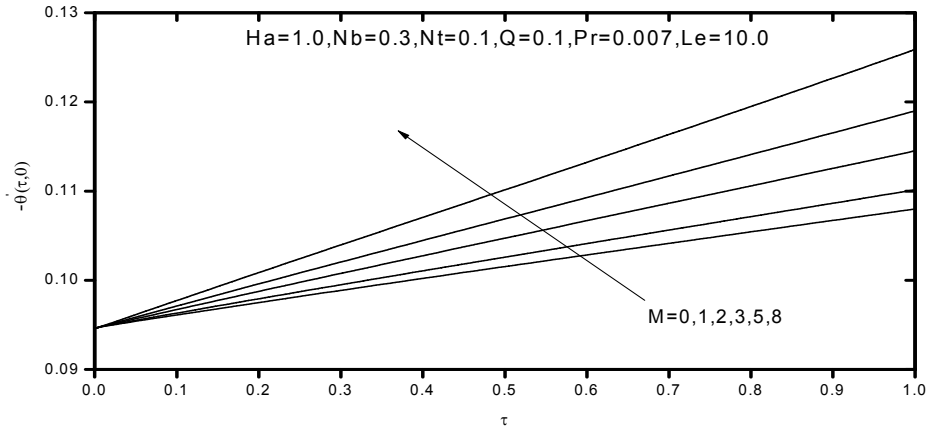

Figure 8: Effects of M on the Nusselt number

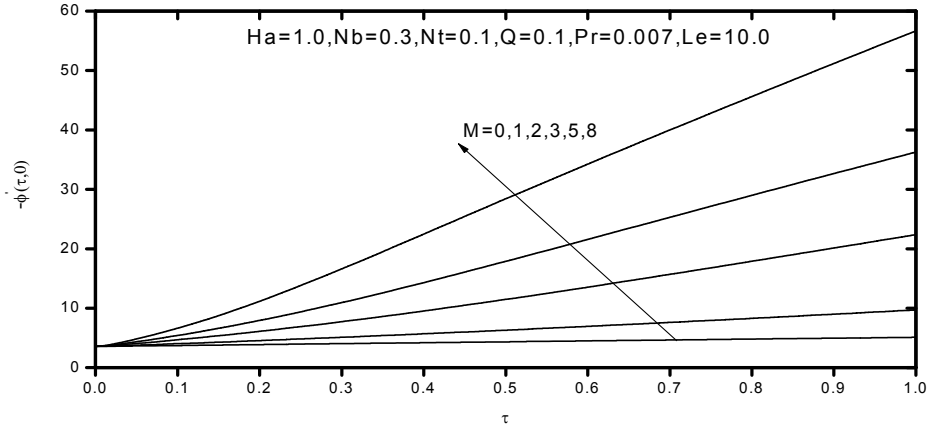

Figure 9: Effects of *M* on the Sherwood number

Figures 10(a)-10(c) depict the influence of increasing the Brownian motion parameter *Nb* on the behavior of the unsteady profiles of velocity, temperature and nanoparticles volume fraction, respectively.

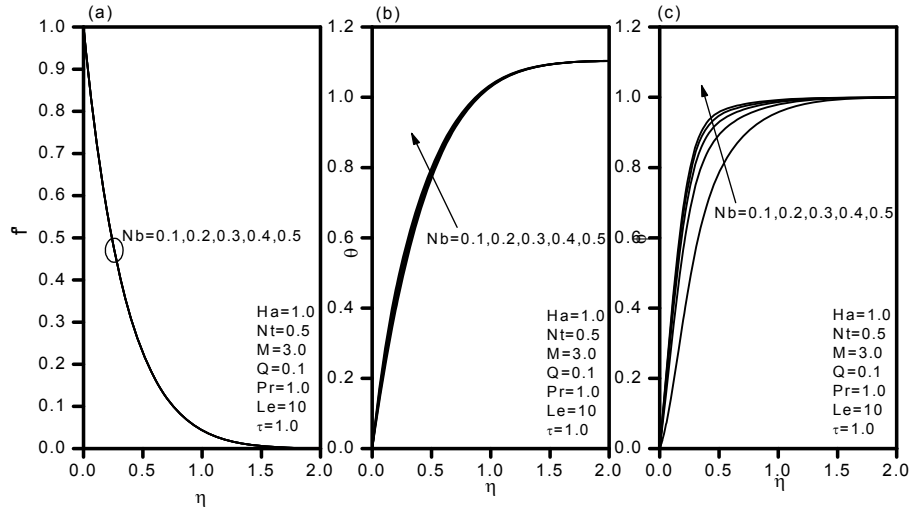

Figure 10: Effects of *Nb* on the (a) velocity, (b) temperature, (c) volume fraction profiles

It can be seen that increasing the value of the Brownian motion parameter *Nb* causes increases in both of the temperature and nanopartciles volume fraction profiles. However, changes in *Nb* do not affect the flow characteristics since the flow problem is independent of the thermal and nanoparticles volume fraction distribution problems. These behaviors are clearly shown in Figures 9(a)-(c).

Figures 11 and 12 present the effects of the Brownian motion parameter *Nb* on the time histories of the Nusselt number *Nu* and the Sherwood number *Sh*, respectively. As indicated before, increasing the Brownian motion parameter Nb causes increases in the temperature and nanoparticles volume fraction profiles without affecting its flow causing the negative wall slope of temperature and nanoparticles volume fraction profiles to increase. This yields enhancement in the local Nusselt and Sherwood numbers. Moreover, it is obvious that the governing equations (7)-(9) are uncoupled. Therefore, changes in the values of *Nb* will cause no changes in the skin-friction coefficient C_f, and for this reason, no figures for this physical parameter are presented herein.

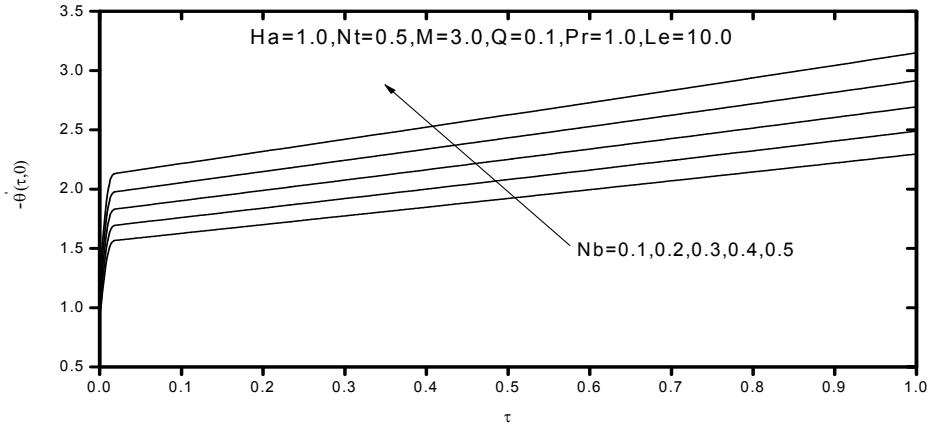

Figure 11: Effects of *Nb* on the Nusselt number

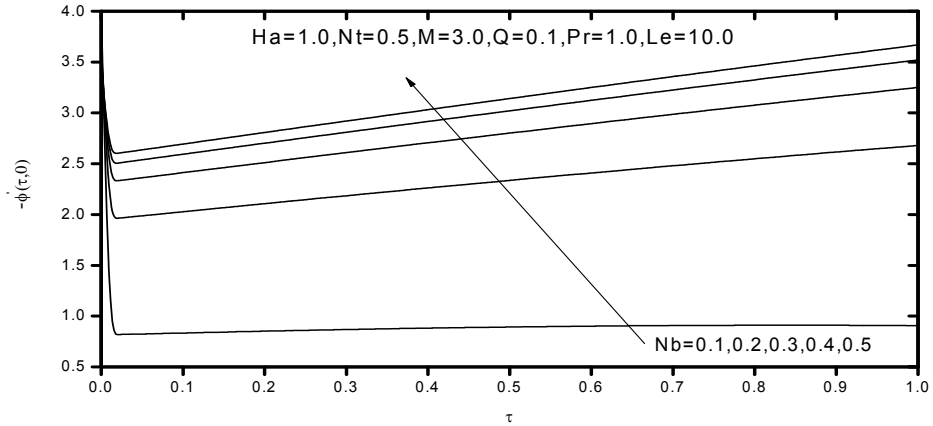

Figure 12: Effects of *Nb* on the Sherwood number

Figures 13(a)-13(c) display typical velocity, temperature and nanoparticles volume fraction profiles for various values of the thermophoresis parameter *Nt*, respectively. Increases in the thermophoresis parameter *Nt* have the tendency to increase the fluid temperature profiles and to decrease the nanoparticles volume fraction profiles without affecting the tangential velocity profiles since the flow problem is uncoupled from the thermal and the nanoparticles volume fraction distribution problems. These behaviors are depicted in the increases in the fluid temperature and decreases in the nanoparticles volume fraction as *Nt* increases shown in Figures 12(b) and 12(c).

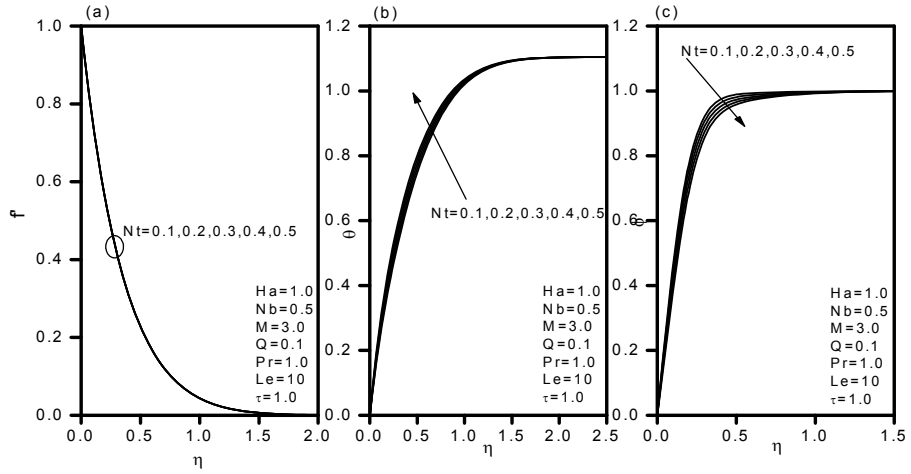

Figure 13: Effects of *Nt* on the (a) velocity, (b) temperature, (c) volume fraction profiles

Figures 14 and 15 depict the influence of the thermophoresis parameter *Nt* on the values of *Nu* and *Sh*, respectively. Increasing the value of the thermophoresis parameter *Nt* results in increasing the temperature while decreasing the volume fraction profiles causing the values of *Nu* to increase and *Sh* to decrease as *Nt* increases.

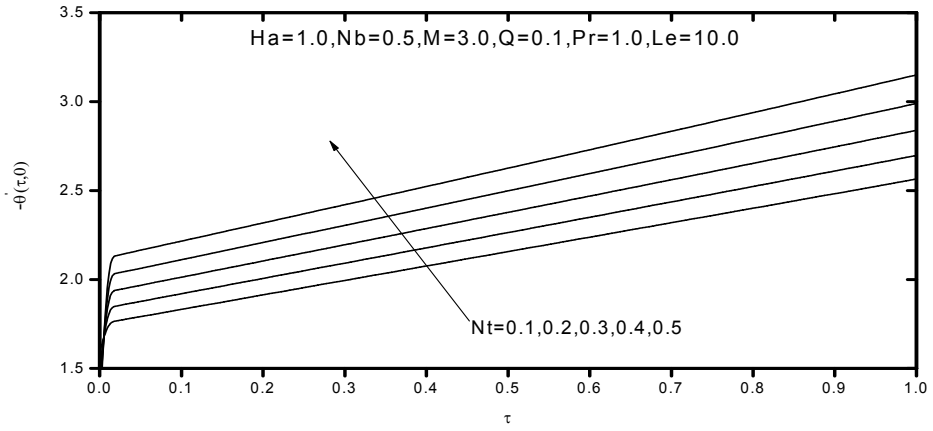

Figure 14: Effects of *Nt* on the Nusselt number

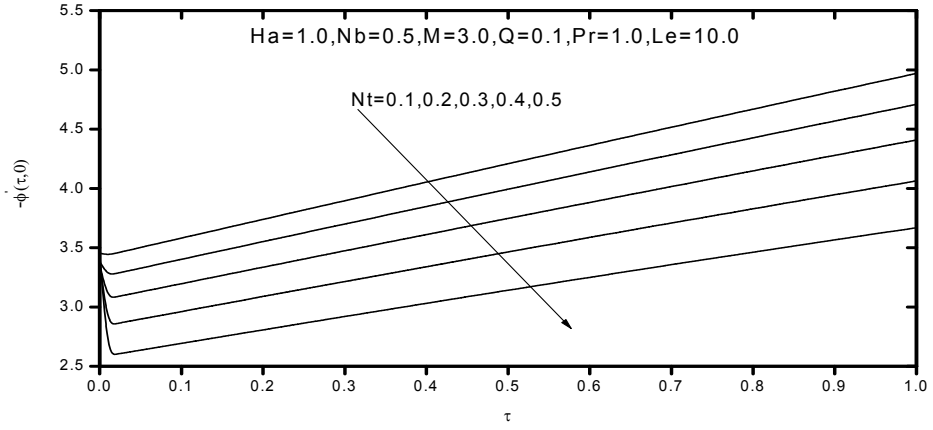

Figure 15: Effects of *Nt* on the Sherwood number

Figures 16(a)-16(c) show the unsteady-state tangential velocity, temperature and nanoparticles volume fraction profiles for different values of the Lewis number *Le*, respectively. It is clearly observed that the fluid temperature decreases while the nanoparticles volume fraction as well as its boundary-layer thickness increase considerably as the Lewis number *Le* increases. This yields enhancements in both heat and mass transfer effects. Moreover, no effect on both of the profiles of fluid tangential velocity for the same uncoupling reason as mentioned above.

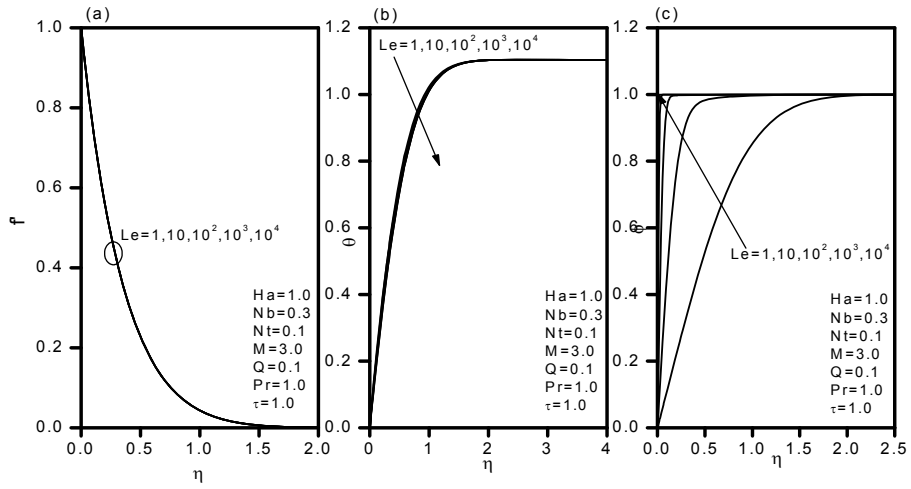

Figure 16: Effects of *Le* on the (a) velocity, (b) temperature, (c) volume fraction profiles

Figures 17 and 18 present the effects of the Lewis number *Le* on the time histories of the Nusselt number *Nu* and the Sherwood number *Sh*, respectively. As mentioned before, increasing the Lewis number *Le* causes enhancements in both the heat and mass transfer effects represented by increases in both of the local Nusselt and Sherwood numbers.

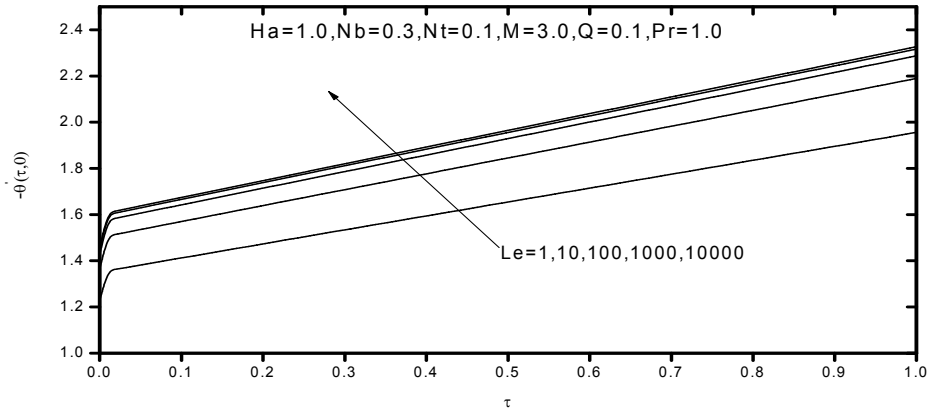

Figure 17: Effects of *Le* on the Nusselt number

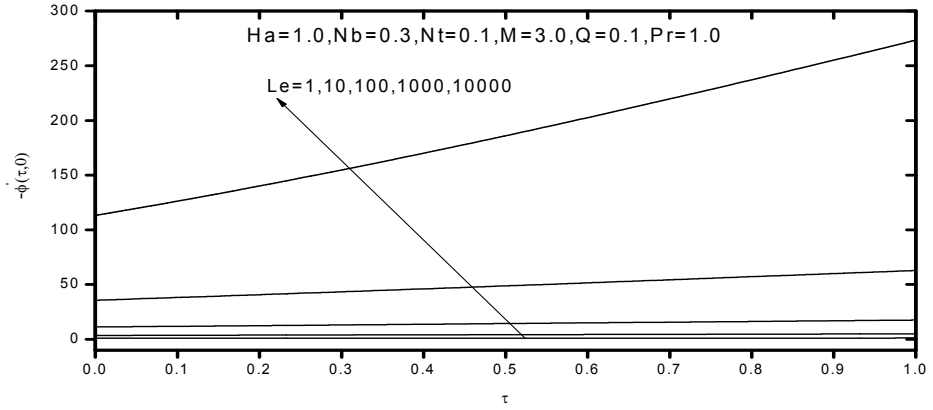

Figure 18: Effects of *Le* on the Sherwood number

Figures 19(a)-19(c) display the effects of the heat generation (Q>0) or absorption (Q<0) parameter on the transient velocity, temperature and nanoparticles volume fraction profiles, respectively. The presence of a heat source (heat generation, Q>0) has the tendency to increase the fluid temperature and the nanoparticles volume fraction. However, the exact opposite behavior occurs in the presence of a heat sink (heat absorption, Q<0) for which the temperature and the nanoparticles volume fraction decrease as Q decreases. These behaviors are depicted in the increases in both of the fluid temperature and the nanoparticles volume fraction profiles as Q increases with pronounced effect on the thermal boundary-layer thickness.

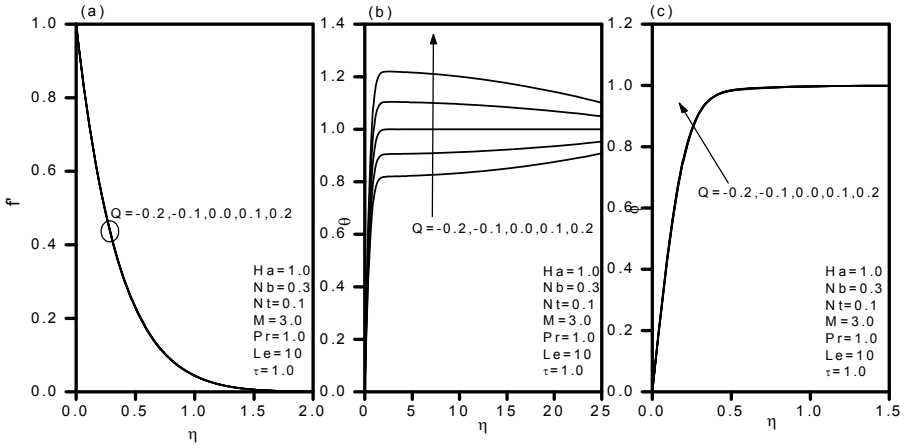

Figure 19: Effects of Q on the (a) velocity, (b) temperature, (c) volume fraction profiles

Finally, Figures 20 and 21 illustrate the effects of the heat generation (Q>0) or absorption (Q<0) parameter on the transient development of the Nusselt and Sherwood numbers (*Nu* and *Sh*), respectively. It is observed that both of the local Nusselt and Sherwood numbers increase as the value of Q increases. In addition, the effect of Q is very small for small values of τ while it is higher for large values of τ.

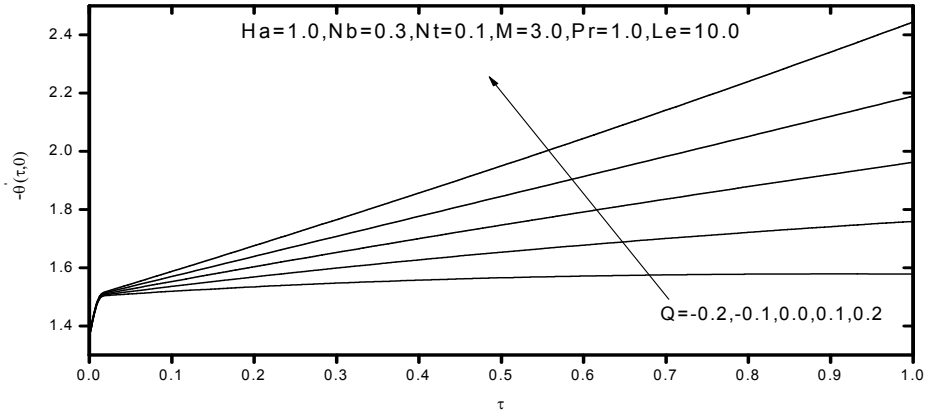

Figure 20: Effects of Q on the Nusselt number

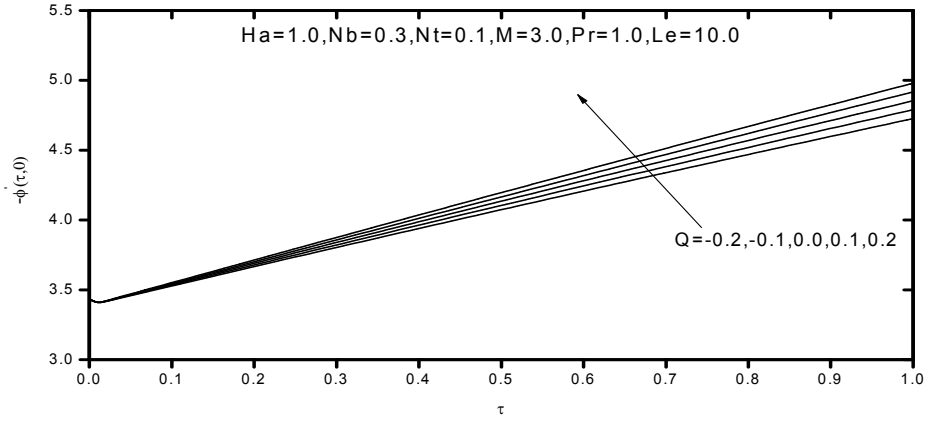

Figure 21: Effects of Q on the Sherwood number

5. Conclusion

The problem of unsteady, laminar, hydromagnetic boundary-layer flow of an electrically-conducting and heat generating or absorbing nanofluid over a horizontal stretching plate in the presence of melting effect was formulated. The model used for the nanofluid incorporates the effects of Brownian motion and thermophoresis. The obtained non-similar differential equations were solved numerically by an efficient implicit finite-difference method. It was found that the skin-friction coefficient increased as either of the Hartmann number or the melting parameter (Stefan number) increased. In addition, the Nusselt number was increased as either of the melting parameter, Brownian motion parameter, thermophoresis parameter, Lewis number or the heat generation coefficient was increased, whereas, it decreased as the strength of the magnetic field was increased. Furthermore, the Sherwood number was increased as the melting parameter, Brownian motion parameter, Lewis number or the heat generation coefficient increased, while the opposite behavior was obtained as the strength of the magnetic field and thermophoresis parameter were increased.

Nomenclature

a constant
B_0 magnetic induction
C nanoparticle volume fraction
C_f skin-friction coefficient
C_s heat capacity of the solid surface
C_w nanoparticle volume fraction at the vertical plate
C_∞ ambient nanoparticle volume fraction attained as y tends to infinity
D_B Brownian diffusion coefficient
D_T thermophoretic diffusion coefficient
f dimensionless stream function
Ha Hartmann number
k thermal conductivity
Le Lewis number
M Stefan number or melting parameter
Nb Brownian motion parameter
Nt thermophoresis parameter
Nu Nusselt number
Pr Prandtl number
Q dimensionless heat generation or absorption coefficient,
Q_0 heat generation or absorption coefficient.
Sh Sherwood number
t time

T temperature
T_m melting temperature
T_s solid surface temperature
T_∞ ambient temperature attained as y tends to infinity
u,v fluid tangential velocity, normal velocity
(x,y) tangential distance, and transverse or normal distance

Greek Symbols:

α thermal diffusivity
σ electrical conductivity
η, τ similarity and non-similarity parameters
χ parameter defined by equation (3)
λ latent heat of the fluid
υ viscosity of the base fluid
θ dimensionless temperature
ϕ dimensionless nano-particle volume fraction
ψ stream function
ρ_f density of the base fluid
ρ_p nano-particle mass density
$(\rho c)_f$ heat capacity of the fluid
$(\rho c)_p$ effective heat capacity of nano-particle material

Subscripts

w conditions at the wall
∞ conditions in the free stream

References

Abu-Nada, E. and Oztop, H.F., "Effects of inclination angle on natural convection in enclosures filled with Cu-water nanofluid", International Journal of Heat and Fluid Flow, 2009, 30, 669-678.

Bakier, A.Y., "Aiding and opposing mixed convection flow in melting from a vertical flat plate embedded in a porous medium", Transport in Porous Media, 1997, 29, 127-139.

Bakier, A.Y., Rashad, A.M. and Mansour, M.A., "Group method analysis of melting effect on MHD mixed convection flow from radiate vertical plate embedded in a saturated porous media", 2009, 14, 2160-2170.

Blottner, F.G., "Finite-difference methods of solution of the boundary-layer equations", AIAA Journal, 1970, 8, 193-205.

Chamkha, A.J., "Unsteady hydromagnetic flow and heat transfer from a non-isothermal stretching sheet immersed in a porous medium", Int. Comm. Heat Mass transfer, 1998, 25, 899-906.

Chamkha, A.J., Ahmed, S.E. and Aloraier, A.S., "Melting and radiation effects on mixed convection from a vertical surface embedded in a non-Newtonian fluid saturated non-Darcy porous medium for aiding and opposing eternal flows", International Journal of the Physical Sciences, 2010, 5 (7), 1212-1224.

Chamkha, A.J., Aly, A.M. and Al-Mudhaf, H., "Laminar MHD mixed convection flow of a nanofluid along a stretching permeable surface in the presence of heat generation or absorption effects", International Journal of Microscale and Nanoscale Thermal and Fluid Transport Phenomena, 2011, 2, Article 3.

Chamkha, A.J., Gorla, R.S.R. and Ghodeswar, K., "Non-similar solution for natural convective boundary layer flow over a sphere embedded in a porous medium saturated with a nanofluid", Transport Porous Medium, 2011, 86, 13-22.

Cheng, W.T. and Lin, C.H., "Unsteady mass transfer in mixed convective heat flow from a vertical plate embedded in a liquid-saturated porous medium with melting effect", International Communications in Heat and Mass Transfer, 2008, 35, 1350-1354.

Choi, S.U.S., "Enhancing thermal conductivity of fluids with nanoparticle. in: Siginer, D.A., Wang, H.P., (Eds.), Developments and Applications of Non-Newtonian Flows", ASME FED, 1995, 231/66, 99-105.

Duangthongsuk, W. and Wongwises, S., "Effect of thermophysical properties models on the predicting of the convective heat transfer coefficient for low concentration nanofluid", International Communications in Heat and Mass Transfer, 2008, 35, 1320-1326.

Epstein, M. and Cho, D.H., "Laminar film condensation on a vertical melting surface", ASME J. Heat Transfer, 1976, 98, 108-113.

Gorla, R.S.R., EL-Kabeir, S.M.M. and Rashad, A.M., "Heat transfer in the boundary layer on a stretching circular cylinder in a nanofluid", Journal of Thermophysics and Heat Transfer, 2011, 25, 183-186.

Gorla, R.S.R., Mansour, M.A., Hassanien, I.A. and Bakier, A.Y., "Mixed convection effect on melting from a vertical plate", Transport in Porous Media, 1999, 36, 245-254.

Hamad, M.A.A., "Analytical solution of natural convection flow of a nanofluid over a linearly stretching sheet in the presence of magnetic field", International Communications in Heat and Mass Transfer, 2011, 38, 487-492.

Hassanien I.A. and Bakier, A.Y., "Melting with mixed convection flow from horizontal flat plate embedded in a porous medium", Earth, Moon, Planets, 1991, 52, 51-63.

Kazmierczak, M., Poulikakos, D. and Sadowski, D., "Melting of a vertical plate in porous medium controlled by forced convection of a dissimilar fluid", Int. Comm. Heat Mass Transfer, 1987, 14, 507-517.

Nield, D.A. and Kuznetsov, A.V., "Thermal instability in a porous medium layer saturated by a nanofluid", International Journal of Heat and Mass Transfer, 2009, 52, 5796-5801.

Nield, D.A. and Kuznetsov, A.V., "The Cheng-Minkowycz problem for natural convective boundary-layer flow in a porous medium saturated by a nanofluid", International Journal of Heat and Mass Transfer, 2009, 52, 5792–5795.

Rana, P. and Bhargava, R., "Numerical study of heat transfer enhancement in mixed convection flow along a vertical plate with heat source/sink utilizing nanofluids", Commun. Nonlinear. Sci. Numer. Simulat., 2011, 16, 4318-4334.

Roberts, L., "On the melting of a semi-infinite body of ice placed in a hot stream of air", J. Fluid Mech., 1958, 4, 505-528.

Walker, G. "A world melting from the top down", Nature, 2007, 446, 718-721.

Wen T. Cheng, C. and Lin, H., "Melting effect on mixed convective heat transfer with aiding and opposing external flows from the vertical plate in a liquid-saturated porous medium", Int. J. Heat and Mass Transfer, 2007, 50, 3026-3034.